Journal of Power Sources 231 (2013) 1–5

Contents lists available at SciVerse ScienceDirect

Journal of Power Sources

journal homepage: www.elsevier.com/locate/jpowsour

Short communication

Theoretical Graetz–Damköhler modeling of an air-breathing microfluidic fuel cell

Jin Xuan [a,b,*], Huizhi Wang [c], Dennis Y.C. Leung [c], Michael K.H. Leung [b,**], Hong Xu [a], Li Zhang [a], Yang Shen [c]

[a] State-Key Laboratory of Chemical Engineering, School of Mechanical and Power Engineering, East China University of Science and Technology, Shanghai, China
[b] Ability R&D Energy Research Center, School of Energy and Environment, City University of Hong Kong, Hong Kong
[c] Department of Mechanical Engineering, The University of Hong Kong, Hong Kong

HIGHLIGHTS

- A theoretical model of air-breathing microfluidic fuel cells (MFC) is reported.
- Pe–Da analysis for MFC is performed.
- Electrode kinetics is important for fuel utilization–current relationship.
- Co-laminar flow of MFC is largely the limiting factor causing low fuel utilization.

ARTICLE INFO

Article history:
Received 27 August 2012
Received in revised form
18 December 2012
Accepted 20 December 2012
Available online 31 December 2012

Keywords:
Microfluidic fuel cell
Analytical model
Fuel utilization
Damköhler number
Graetz number

ABSTRACT

This paper reports the first theoretical modeling study of air-breathing microfluidic fuel cells (MFCs). The model is based on a semi-empirical Graetz–Damköhler (Gz–Da) analysis. The theoretical formulas derived clearly demonstrate the effects of the MFC design and operational parameters on the electrochemical activities of MFCs in quantitative detail. The modeling analysis shows that the electrode kinetics have significant effects on the trade-off relationship between the fuel utilization and current density. Moreover, the analysis reveals that the co-laminar flow of MFCs limits the fuel utilization considerably.

1. Introduction

Air-breathing, membrane-less, microfluidic fuel cells (MFCs) fed with liquid fuels, such as formic acid, methanol, and ethanol, are highly promising as a portable electricity supply for microelectronics due to their high energy density and simple cell structure [1,2]. The operation of a MFC without a membrane has many potential benefits, such as low cost, simple assembly and easy water management over the operation of common proton exchange membrane fuel cells (PEMFCs) and direct methanol fuel cells (DMFCs) that rely on Nafion® membranes [1–5]. Widely reported R&D efforts on MFCs have been summarized in recent review papers [2,6]. One of the major challenges for further development of MFCs is to gain a better understanding of the underlying principles governing the micro-scale interactions between the microfluidic hydrodynamics and electrochemical kinetics. Previous numerical modeling studies performed by other researchers [3,4] and us [7,8] have provided some knowledge of the MFC phenomena and comprehensive descriptions of the physicochemical processes in MFCs. Yet, the present literature lacks theoretical and analytical modeling work that can give more insight into the principles governing the complex mechanisms in MFCs. Moreover, analytical solutions can facilitate effective engineering analyses for practical fuel cell design, optimization and operational control. In this study, we report a theoretical study of MFC fuel utilization and

* Corresponding author. State-Key Laboratory of Chemical Engineering, School of Mechanical and Power Engineering, East China University of Science and Technology, Shanghai, China. Tel.: +86 21 64252847; fax: +86 21 64253810.
** Corresponding author. Tel.: +852 3442 4626; fax: +852 3442 0688.
E-mail addresses: jxuan@ecust.edu.cn (J. Xuan), mkh.leung@cityu.edu.hk (M.K.H. Leung).

0378-7753/$ – see front matter © 2012 Elsevier B.V. All rights reserved.
http://dx.doi.org/10.1016/j.jpowsour.2012.12.090

current–potential characteristics based on semi-empirical derivations. It is found that complex diffusion–convection–reaction interactions in MFCs can be described well by two dimensionless variables, the Damköhler (Da) and Graetz (Gz) numbers.

2. Model development

The schematic of a MFC is shown in Fig. 1. In a state-of-the-art air-breathing MFC [1,6], the anode and cathode are placed at the opposite walls of the microchannel. The cathode is a porous gas diffusion electrode, which commonly consists of carbon papers. The cathode catalyst is coated on the inside of the carbon paper to form an electrode–electrolyte reactive interface. Oxygen in the air can diffuse from the ambient environment to the reaction site [7,8]. The transport of the fuel species at the anode half-cell is governed by the general conservation equation,

$$-\nabla\cdot\vec{N}_i = -\nabla\cdot\left(\vec{v}\,c_i - D_i\nabla c_i\right), \tag{1}$$

where c_i, N_i, $\vec{v}$, and D_i denote the species concentration (mol m^{-3}), surface reaction flux (mol m^{-2} s^{-1}), velocity (m s^{-1}) and diffusion coefficient (m^2 s^{-1}), respectively. For the anode electrochemical reaction, the boundary condition on the molar flux at the electrode surface is

$$\vec{u}\cdot\vec{N} = R_\mathrm{a}, \tag{2}$$

where $\vec{u}$ is the surface unit vector (inward) and R_a is the anode electrochemical reaction rate (mol m^{-3} s^{-1}). The Tafel law can be employed to determine R_a for most of the fuels used in MFCs (e.g., formic acid, methanol, etc.),

$$R_\mathrm{a} = \frac{J}{nF} = R_{a,0}c_i^{\gamma}\exp\left(\frac{\alpha nF\eta_a}{RT}\right), \tag{3}$$

where $R_{\mathrm{a},0}$ is the anode reaction rate corresponding to the exchange current density ($J_{\mathrm{a},0}$) and J is the electrode current density (A m^{-2}). The n, F, γ, α, η_a, T and R symbols denote the charge transfer number, Faraday constant (96,500 s A mol^{-1}), reaction order, charge-transfer coefficient, anode overpotential (V), temperature (K), and the universal gas constant, respectively.

Two dimensionless numbers, namely the Graetz (Gz) number and Damköhler (Da) number, are employed for parametric correlation analysis. The Graetz (Gz) number is defined as the ratio of the time scale of diffusion to that of convection,

$$\mathrm{Gz} = \frac{\bar{t}_\mathrm{d}}{\bar{t}_\mathrm{c}} = \frac{L_\mathrm{c}D_i}{UL_\mathrm{d}^2}, \tag{4}$$

where L_c and L_d are the length scales for convection and diffusion transport, respectively. For MFCs in particular, L_c represents the electrode length, and L_d is the reactant stream width. U is the inlet velocity of the fuel and catholyte (m s^{-1}). The Damköhler (Da) number is the ratio of the maximum surface reaction rate (e.g., the electrode reaction) to the rate of reactant transport to the surface,

$$\mathrm{Da} = \frac{k_\mathrm{c}c_0^{\gamma-1}L_\mathrm{d}}{D_i}, \tag{5}$$

where k_c is the reaction rate constant and c_0 is the bulk concentration. For chemical reactions, k_c is usually determined by the Arrhenius law. In an electrochemical system, i.e., a MFC, the surface reaction rate is usually presented in terms of the current density, and the global electrode kinetics is usually expressed via the Tafel equation (Eq. (3)). Thus, the Da number for MFCs becomes a function of the electrode overpotential,

$$\mathrm{Da_{MFC}} = \frac{R_{\mathrm{a},0}c_0^{\gamma-1}L_\mathrm{d}}{D_i}\exp\left(\frac{\alpha nF\eta_\mathrm{a}}{RT}\right). \tag{6}$$

Assuming that the hydrodynamics of a MFC channel is a fully developed laminar flow, the dimensionless bulk concentration (c_i/c_0) is a function of Da and Gz and can be determined analytically according to Gervais et al. [9]:

$$\frac{c_i}{c_0} = \exp\left(-\frac{\lambda_1^2}{6}\mathrm{Gz}\right), \tag{7}$$

where the first eigenvalue, λ_1, is numerically fitted to the form in [9],

$$\frac{\lambda_1^2}{6} = 3.2608(1-\exp(-0.68\,\mathrm{Da})) + 4.28\exp\left(\frac{-6.1}{\mathrm{Da}}\right). \tag{8}$$

Once the bulk concentration at the outlet is known, the reactant conversion rate (C_f), which is an important parameter for the evaluation of the cell performance, can be calculated from the following equation,

$$C_\mathrm{f} = \frac{c_0 - c_i}{c_0}. \tag{9}$$

Assuming that the internal ohmic resistance of the anode is negligible, the current density of the cell can be derived from Faraday's law,

$$J = \frac{nFQC_\mathrm{f}}{S_\mathrm{electrode}} = \frac{nFc_0UL_\mathrm{d}C_\mathrm{f}}{L_\mathrm{c}}, \tag{10}$$

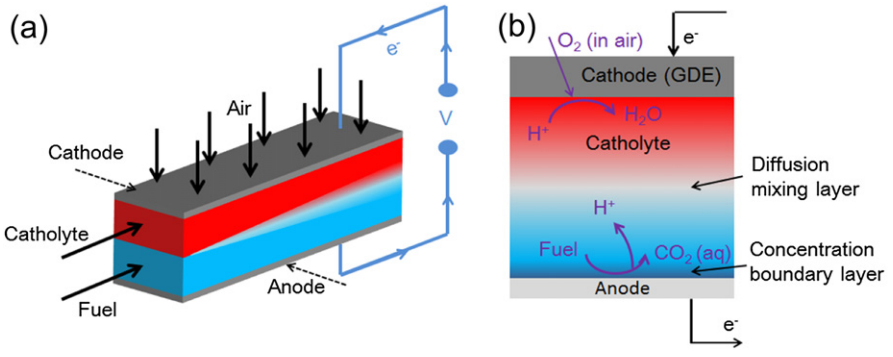

Fig. 1. (a) Schematic illustration of a microfluidic fuel cell; (b) cross-sectional view of a MFC.

where $S_{electrode}$ is the reactive area of the electrode (m^2). Further, we can derive two useful analytical expressions. First, the normalized current density can be written as a function of Gz and Da:

$$J^* = 1 - \exp\left[-\left(3.2608(1-\exp(-0.68\,\mathrm{Da})) + 4.28\exp\left(\frac{-6.1}{\mathrm{Da}}\right)\right)\mathrm{Gz}\right], \quad (11)$$

where J^* is defined as

$$J^* = J\frac{L_c}{nFc_0UL_d}. \quad (12)$$

Second, the absolute value of J as a function of the anode overpotential can be derived by substituting Eq. (6) into Eq. (10),

$$J = \frac{nFc_0UL_d}{L_c}\left\{1-\exp\left[-\left(3.2608\left(1-\exp\left(-0.68\frac{R_{a,0}L_d}{D_i}\exp\left(\frac{\alpha nF\eta_a}{RT}\right)\right)\right)+4.28\exp\left(\frac{-6.1D_i}{R_{a,0}L_d}\exp\left(\frac{-\alpha nF\eta_a}{RT}\right)\right)\right)\frac{L_cD}{UL_d^2}\right]\right\}. \quad (13)$$

So far, an analytical expression of the transport-reaction interactions at the anode has been derived. Based on this expression, we can predict the whole-cell performance, i.e., the J–V relationship for MFCs under various design and operating conditions. The polarization characteristics of the air-breathing cathode, which are independent of the microchannel design and hydrodynamic conditions, can be obtained from experimental data [10,11]. Here, we use a Tafel fit to express the cathode kinetics,

$$\eta_c = A_c \ln\left(\frac{J}{J_{c,0}}\right), \quad (14)$$

where A_c is the Tafel slope (V) at the cathode, η_c is the cathode overpotential (V) and $J_{c,0}$ is the cathode exchange current density (A m^{-2}). The electrolyte ohmic overpotential (η_o) can be expressed as

$$\eta_o = JR_{electrolyte}, \quad (15)$$

where $R_{electrolyte}$ is the electric resistance of the electrolyte (Ω). Finally, the J–V relationship, which is the most important performance metric of a fuel cell, can be obtained from

$$V = E^0 - \eta_a - \eta_c - \eta_o, \quad (16)$$

where E^0 is the reversible potential (V). The η_a, η_c and η_o values can be derived from Eqs. (13)–(15), respectively.

3. Results and discussion

We first validate the present theoretical model by comparing the analytical results to experimental measurements and numerical modeling data. The input parameters used in the model are summarized in Table 1. Fig. 2(a) and (b) shows the comparison between the analytical results and the experimental data [12] for the electrode polarization and J–V characteristics of the cell, respectively. A large deviation of 17% between the analytical results and the experimental data is found at a single data point near J = 50 mA cm^{-2}. At all other points, all of the curves show reasonable agreement (deviations less than 8%). Fig. 2(c) plots the theoretical J–V curves of the cell at different inlet velocities.

Table 1
Basic input parameters used in the model.

Parameters	Value	References
Cell geometry		
L_c	20.5 mm	[12]
L_d	2 mm	[12]
Electrode kinetics		
$J_{a,0}$	1.5×10^{-5} mA cm^{-2}	[13]
$J_{c,0}$	0.1 mA cm^{-2}	Fitted
γ	1	[7,8]
α	0.5	[7,8]
n	1	[7,8]
A_c	0.0865 V	Fitted
Operating conditions		
U	1.6 mm s^{-1}	[12]
c_0	1 M	[12]

The changes in the performance characteristics between the three operating regimes (i.e., activation, ohmic and concentration regimes) are captured well, indicating that the convection–diffusion–reaction interactions during the MFC operation are accurately predicted by the theoretical model. Moreover, a linear relationship is found between the cube root of the predicted limiting current and the inlet velocity (the inset in Fig. 2(c)), which is consistent with the one-third power law derived from the theory and experiment [14]. Furthermore, the cell performance obtained from the theoretical model and our previous numerical model [7,8,15] are comparable over a wide range of the operating current density as shown in Fig. 2(d). The deviation between the analytical and numerical modeling results is less than 10%, illustrating the good agreement between the two sets of modeling results. The model validation indicates that the present theoretical model would be an effective tool to predict the electrochemical activities of MFCs with similar cell designs.

We then use the model to extract the most important governing laws for the complex underlying physico-electrochemical interactions. The dimensionless numbers, Da and Gz, indicate the relative importance of convection, diffusion and electrochemical reaction in MFCs. The Gz number reveals whether the operating region is an “entrance region” or a “fully developed region.” For Gz < 1, a portion of the reactant stream does not have sufficient time to reach the reactive surface before leaving the microchannel, resulting in the formation of a concentration boundary layer next to the electrode. On the other hand, for Gz > 1, the reactants have sufficient time to reach the reactive surface, and the reactants are depleted in the bulk. The Da number shows whether the operating region is “kinetically controlled” or “transport-controlled”. For Da > 1, the reaction rate is fast compared to the rate of the reactant transport to the catalyst site, and the transport rate reaches a maximum at the reactive surface where the concentration is approximately zero [9]. Therefore, the current density is limited by the transport rate (i.e., commonly known as “limiting current behavior”). For Da < 1, the transport of the reactant species is faster than the reaction rate. The fuel concentration at the electrode surface is not zero, and the electrode kinetics determine the overall reaction rate. This behavior can be found in the activation regime during the MFC operation. As a result, four regions of operating conditions for MFCs can be conceptually defined in a Gz–Da coordinate system as shown in Fig. 3. The origin of the Gz–Da coordinate system is Gz = 1, Da = 1. The two axes divide the whole domain into four regions, i.e., an entrance kinetically controlled region (Gz < 1, Da < 1), entrance transport-controlled region (Gz < 1, Da > 1), fully developed kinetically controlled region (Gz > 1, Da < 1), and fully developed transport-controlled region (Gz > 1, Da > 1).

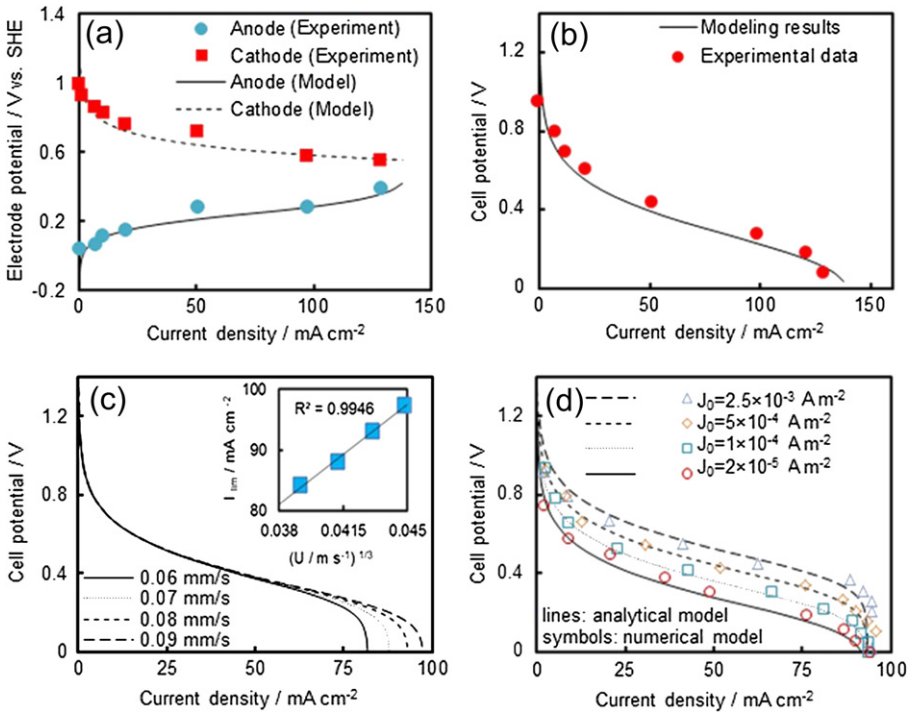

Fig. 2. Model validation: comparison of the analytical results and experimental data [8] for the (a) electrode polarization curves and (b) J–V curve of the cell; (c) analytical results for the J–V curves of the cell at different inlet velocities (inset: cube root of the predicted limiting current vs. inlet velocity); (d) comparison of the analytical model and the numerical model.

The variation of the dimensionless current, J^*, in the Gz–Da coordinate system is calculated using the theoretical model and plotted in Fig. 3. The results provide a general picture on the cell performance under various co-effects of Gz and Da. It can be found that operating a MFC in the fully developed transport-controlled region yields the highest J^* value. The effects of the Gz–Da interaction on the MFC performance are further discussed below.

The trade-off between the current density and fuel utilization during the operation of a MFC has been extensively studied [6,16,17]. However, the role of the electrode kinetics on the trade-off relationship has not been previously explored. Fig. 4(a) shows the trade-off curves between C_f and J at different Da values. It is found that the electrode kinetics (as reflected by Da) have a significant effect on the trade-off between the fuel utilization and current density. The C_f–J trade-off curve decreases faster at lower Da values, indicating that the cell performance suffers from more serious trade-off limitations when the electrode is less reactive. The first derivatives of the three C_f–J trade-off curves, representing the rates of decline of the curves, are calculated and compared in the inset in Fig. 4(a). With an increase in the current density, the rate of decline of the C_f–J curve linearly increases, which implies that the trade-off problem becomes much more severe at higher operating current densities. The results show that although the trade-off problem between the fuel utilization and current density is hardly avoidable during the operation of a MFC, we can optimize Da and Gz during the cell design and operation to reduce the rate of decline of the C_f–J curve and thus achieve a higher fuel utilization with a minimal loss in the cell current density.

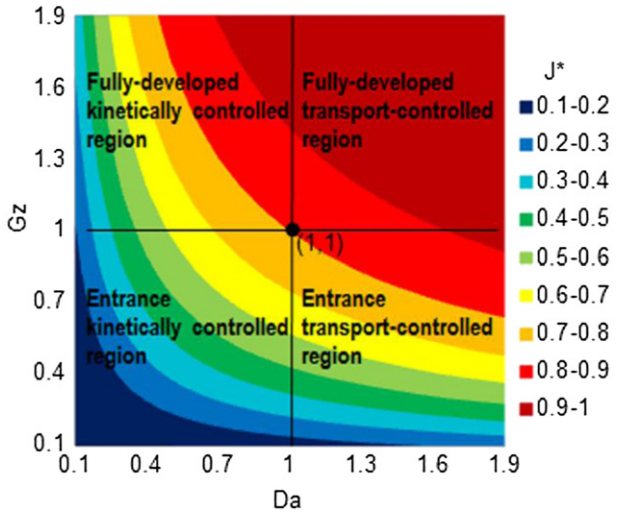

Fig. 3. Effects of Gz and Da on the dimensionless current, J^*, of a MFC.

According to the above Da–Gz analysis of the MFC performance (i.e., Figs. 3 and 4(a)), high fuel utilization (near 100%) seems theoretically achievable when the cell operates at high Gz and Da values. Yet, in reality, the reported fuel utilization in MFCs is very poor, commonly lower than 10% [16,17]. Here, we attempt to use the Gz–Da analysis to explain why high fuel utilization in MFCs is unachievable in practice. For the Gz number, the maximum convectional time scale of the electrode reaction is limited by the time required to achieve full mixing of the two streams, i.e., the diffusion time scale ($\bar{t}_{c,max} = \bar{t}_m$). Because the time scales for a molecule at the stream interface to diffuse across the designated electrode and across the counter electrode are identical ($\bar{t}_d = \bar{t}_m$), Gz cannot theoretically be greater than 1 for the co-laminar MFC. The butterfly effect caused by an uneven velocity distribution inside the microchannel [6] further reduces the Gz number that can be achieved during cell operation in practice, making it lower than 0.2 under normal conditions. The Da number, on the other hand, is determined by several parameters according to Eq. (6), i.e., j_0 (10^{-5} to 1 A m^{-2}), η_a (0.1–0.5 V) and L_d (0.2–1 mm). Based on the possible ranges of these parameters, 0.1–5 is a reasonable value for Da. The limited values of Da and Gz that can be achieved in practice result in low fuel

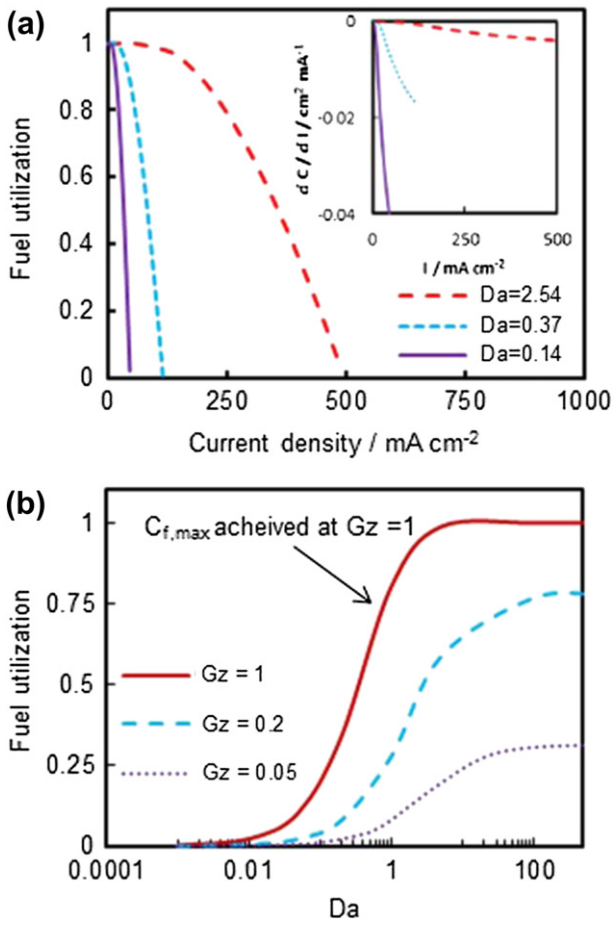

Fig. 4. (a) C_f vs. J for different Da values (inset: first derivatives of the three C_f–J trade-off curves); (b) MFC fuel utilization for different Gz and Da values.

utilization. Fig. 4(b) plots the MFC fuel utilization for different Gz and Da values. It is found that for a given Gz value, increasing Da leads to an increase in the fuel utilization, but the fuel utilization ultimately reaches a plateau. On the other hand, for a given Da value, an increase in Gz might also improve the fuel utilization, but the enhancement is restricted by the upper limit of $Gz = 1$ (theoretically) or $Gz \approx 0.2$ (in practice). As shown in Fig. 4(b), for $Gz < 0.2$ and $Da < 5$, the maximal achievable fuel utilization is approximately 50%. For a more commonly used Gz value of less than 0.05, the maximal achievable fuel utilization is only approximately 15%. This analysis explains the reason why the fuel utilization in MFCs has previously been reported to be low. It also suggests that because of the co-laminar MFC structure, the possibilities for improving the fuel utilization are largely limited. To achieve a breakthrough in the fuel utilization in MFCs (i.e., near 100%), microfluidic network or electrode arrangement designs for MFCs need to be explored. Some new MFC designs, such as counter-flow networks for fuel and oxidant streams [18] and flow-through porous electrodes [19], have shown promise for achieving a much higher fuel utilization than the conventional co-laminar flow-based MFCs.

4. Conclusions

In this study, a theoretical model for MFCs has been successfully derived using semi-empirical expressions and subsequently validated against experimental and numerical data. The dependence of the MFC fuel utilization and J–V characteristics on the cell design and operating parameters are clearly shown in the formulas derived here. Therefore, the present theoretical model is more advantageous than previous numerical models because insights into the operation of MFCs can be obtained directly from the theoretical formulas. The analytical results could serve as a ready-to-use engineering tool to guide the design and control of MFCs.

In addition, based on the analytical model, a Graetz–Damköhler (Gz–Da) analysis is performed to study the relative importance of convection, diffusion and surface reactions during the operation of MFCs and their effects on the cell performance. It is found that the electrode kinetics have a significant effect on the trade-off relationship between the fuel utilization and current density of MFCs. Moreover, it is revealed that the co-laminar flow structure of MFCs largely limits the cell performance by prohibiting high fuel utilization.

Acknowledgments

The research work presented in this paper was funded by the Ability R&D Energy Research Centre under the School of Energy and Environment at the City University of Hong Kong, a CityU Start-up Grant (7200297), the Shanghai Pujiang Program (12PJ1402100) and the Fundamental Research Funds for the Central Universities, P.R. China.

References

[1] S.A.M. Shaegh, N.T. Nguyen, S.H. Chan, J. Power Sources 209 (2012) 312–317.
[2] E. Kjeang, N. Djilali, D. Sinton, J. Power Sources 186 (2009) 353–369.
[3] S.A.M. Shaegh, N.T. Nguyen, S.H. Chan, J. Micromech. Microeng. 20 (2010) 105008.
[4] D. Krishnamurthy, E.O. Johansson, J.W. Lee, E. Kjeang, J. Power Sources 196 (2011) 10019–10031.
[5] Nature 438 (2005) 399.
[6] S.A.M. Shaegh, N.T. Nguyen, S.H. Chan, Int. J. Hydrogen Energy 36 (2011) 5675–5694.
[7] H. Wang, D.Y.C. Leung, J. Xuan, Int. J. Hydrogen Energy 36 (2011) 14704–14718.
[8] J. Xuan, D.Y.C. Leung, M.K.H. Leung, M. Ni, H. Wang, Int. J. Hydrogen Energy 36 (2011) 9231–9241.
[9] T. Gervais, K.F. Jensen, Chem. Eng. Sci. 61 (2006) 1102–1121.
[10] F.R. Brushett, R.S. Jayashree, W.P. Zhou, P.J.A. Kenis, Electrochim. Acta 54 (2009) 7099–7105.
[11] R.S. Jayashree, D. Egas, D. Natarajan, J.S. Spendelow, L.J. Markoski, P.J.A. Kenis, Electrochem. Solid State Lett. 9 (2006) A252–A256.
[12] R.S. Jayashree, L. Gancs, E.R. Choban, A. Primak, D. Natarajan, L.J. Markoski, P.J.A. Kenis, J. Am. Chem. Soc. 127 (2005) 16758–16759.
[13] F.A. Viva, Studies on direct methanol, formic acid and related fuel cells in conjunction with the electrochemical reduction of carbon dioxide, PhD thesis, University Of Southern California, 2009.
[14] E. Kjeang, J. McKechnie, D. Sinton, N. Djilali, J. Power Sources 168 (2007) 379–390.
[15] J. Xuan, M.K.H. Leung, D.Y.C. Leung, H. Wang, Appl. Energy 90 (2012) 87–93.
[16] R. Jayashree, S.K. Yoon, F.R. Brushett, P.O. Lopez-Montesinos, D. Natarajan, L.J. Markoski, P.J.A. Kenis, J. Power Sources 195 (2010) 3569–3578.
[17] D.H. Ahmed, H.B. Park, H.J. Sung, J. Power Sources 185 (2008) 143–152.
[18] J. Xuan, D.Y.C. Leung, M.K.H. Leung, H. Wang, M. Ni, J. Power Sources 196 (2011) 9391–9397.
[19] E. Kjeang, R. Michel, D.A. Harrington, N. Djilali, D. Sinton, J. Am. Chem. Soc. 130 (2008) 4000–4006.